

**Technical Report
1107**

Asymptotic Error for Windowed Discrete Fourier Transforms

A.F. Yegulalp

25 August 2006

Lincoln Laboratory
MASSACHUSETTS INSTITUTE OF TECHNOLOGY
LEXINGTON, MASSACHUSETTS



Prepared for the Defense Advanced Research Projects Agency under
Air Force Contract FA8721-05-C-0002.

Approved for public release; distribution is unlimited.

ADA 452964

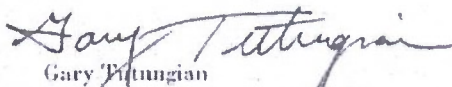
This report is based on studies performed at Lincoln Laboratory, a center for research operated by Massachusetts Institute of Technology. This work was sponsored by the Defense Advanced Research Projects Agency, IXO, under Air Force Contract FA8721-05-4-0002.

This report may be reproduced to satisfy needs of U.S. Government agencies.

The ESC Public Affairs Office has reviewed this report, and it is releasable to the National Technical Information Service, where it will be available to the general public, including foreign nationals.

This technical report has been reviewed and is approved for publication.

FOR THE COMMANDER



Gary Pittungian
Administrative Contracting Officer
Plans and Programs Directorate
Contracted Support Management

Non-Lincoln Recipients

PLEASE DO NOT RETURN

Permission has been given to destroy this document when it is no longer needed.

**Massachusetts Institute of Technology
Lincoln Laboratory**

Asymptotic Error for Windowed Discrete Fourier Transforms

*A.F. Yegulalp
Group 103*

Technical Report 1107

25 August 2006

Approved for public release; distribution is unlimited.

Lexington

Massachusetts

ABSTRACT

The windowed discrete Fourier transform (DFT) is a widely used tool in countless signal processing applications. Surprisingly, there has been little analysis of its accuracy for the processing of random bandlimited signals. This report derives an error formula at leading asymptotic order in the number of data samples. The formula applies to essentially any window function, with explicit results tabulated for some of the most common cases. The asymptotic error is shown to agree well with Monte Carlo results, even for very small numbers of samples.

TABLE OF CONTENTS

	Page No.
Abstract	iii
List of Illustrations	vii
List of Tables	ix
1. INTRODUCTION	1
2. DEFINITION OF THE PROBLEM	3
3. EVALUATION OF EXPECTATION VALUES	5
4. LEADING ORDER ASYMPTOTICS	7
5. RESULTS FOR FLAT SPECTRAL DENSITY	9
5.1 Evaluation of $Q_p(z)$	9
5.2 Qualitative Description of Error	10
5.3 Evaluation of N_w for Standard Window Functions	11
5.4 Verification of Asymptotic Results	11
6. CONCLUSIONS	19
APPENDIX A: MATHEMATICA CODE FOR GENERATING ASYMPTOTIC RESULTS	21
REFERENCES	27

LIST OF ILLUSTRATIONS

Figure No.		Page No.
1	Plot of the function $Q_p(z)$.	13
2	Normalized mean squared error versus number of samples in window.	14
3	Normalized mean squared error versus number of samples in window.	15
4	Normalized mean squared error for the Hamming window.	16
5	Normalized mean squared error for the Kaiser window ($\beta = 5$).	17
6	Normalized mean squared error versus frequency.	18
A-1	Transcript of Mathematica.	22

LIST OF TABLES

Table No.		Page No.
1	Parameters for Some Standard Window Functions	12

1. INTRODUCTION

Digital signal processing is largely founded on the Nyquist theorem, which tells us that a bandlimited signal can be recovered from its unaliased, discrete samples. The Nyquist theorem makes it possible for a calculation based on discretely sampled data to exactly match one based on continuous quantities. A good example is the Fourier transform of a bandlimited signal $s(t)$:

$$\int_{-\infty}^{\infty} s(t) e^{-2\pi i \mu t} dt = \Delta t \sum_{n=-\infty}^{\infty} s(n\Delta t) e^{-2\pi i \mu n \Delta t}. \quad (1)$$

The equality is exact when $\Delta t \leq \Delta t_{\text{nyq}}$, where Δt_{nyq} is the Nyquist time step.

Unfortunately, Equation (1) does not apply to practical computations since it uses an infinite number of samples. Finite-duration signals cannot be exactly bandlimited, so there must be some amount of aliasing. A common approach is to use a smooth windowing function $w(\tau)$ to select a finite time interval T from the bandlimited signal:

$$\int_{-\infty}^{\infty} s(t) w\left(\frac{t}{T}\right) e^{-2\pi i \mu t} dt \approx \Delta t \sum_{n=-\infty}^{\infty} s(n\Delta t) w\left(\frac{n\Delta t}{T}\right) e^{-2\pi i \mu n \Delta t}. \quad (2)$$

The window function $w(\tau)$ is assumed to be real, non-negative, and strictly zero when $|\tau| > 1/2$. If one is free to use long time intervals T and a smooth window function, the error in Equation (2) can easily be made very small. On the other hand, in certain applications it is likely that T will be modest or small, in which case the error may be significant. One example of such an application is joint time-frequency analysis: one can be forced to use short time windows when the signal has rapidly changing spectral content [1].

Another example, which was the original motivation for this work, is the development of an efficient backprojection image formation algorithm for synthetic aperture radar [2,3]. The algorithm achieves efficiency by decomposing the synthetic aperture integration into a nested hierarchy of synthetic apertures. Maximum efficiency is achieved when the bottom layer of the hierarchy consists of integration over synthetic apertures of only a few Nyquist samples. Thus, algorithmic efficiency forces one into the case where the error in Equation (2) is likely to be significant.

The error in Equation (2) may also be of concern in applications where the required accuracy is very stringent. A common example is adaptive array processing where one wishes to cancel very strong interference sources in order to detect a weak signal of interest. The error incurred in the finite sum of Equation (2) will act like a noise source which scales with the strength of the strongest signals. Successful detection will require that the error be smaller than the ratio of the weak signal to the strong interference.

In [4], the authors consider a version of Equation (2) with a square window function. An exact error expression is computed for deterministic signals with piecewise polynomial structure. For more general classes of deterministic signals, the same error expression is shown to hold in the

limit where $\Delta t \rightarrow 0$ and $\mu \rightarrow \infty$ while $\mu\Delta t$ is held fixed. While the results are mathematically correct, they are not useful for the typical signal processing scenarios because they do not capture the effects of a finite number of data samples. For example, the error is exactly zero for the zero frequency component.

In this report, the signal $s(t)$ is treated as a stochastic quantity and arbitrary window functions $w(\tau)$ are allowed. The mean squared error in Equation (2) is computed at leading asymptotic order in the number of samples $N = T/\Delta t$. Explicit results are given for many common window functions. The error estimates are shown to agree well with Monte Carlo results, even when the number of samples is relatively small.

2. DEFINITION OF THE PROBLEM

Let $s(t)$ be a random signal of bandwidth B , with Fourier transform $S(\nu)$:

$$s(t) = \int_{-\infty}^{\infty} S(\nu) e^{2\pi i \nu t} d\nu \quad (3)$$

$$S(\nu) = 0 \text{ for } |\nu| > \frac{B}{2} \quad (4)$$

The signal $s(t)$ is assumed to be stationary with zero mean and spectral density $\rho(\nu)$:

$$E[s(t)] = 0$$

$$E[s(t)s(t')^*] = \int_{-B/2}^{B/2} \rho(\nu) e^{2\pi i \nu(t-t')} d\nu \rho(\nu) = 0 \text{ for } |\nu| > \frac{B}{2} \quad (5)$$

The windowed Fourier transform is given by the integral

$$I = \int_{-\infty}^{\infty} s(t) w\left(\frac{t}{T}\right) e^{-2\pi i \mu t} dt, \quad (6)$$

where the unit-interval window function $w(\tau)$ is assumed to be real, non-negative, and strictly zero when $|\tau| \geq \frac{1}{2}$. The frequency μ is assumed to be restricted to the interval $|\mu| \leq \frac{B}{2}$. The discrete approximation to the above integral is given by

$$I_D = \Delta t \sum_{n=-\infty}^{\infty} s(t_n) w\left(\frac{t_n}{T}\right) e^{-2\pi i \mu t_n}, \quad (7)$$

where $t_n = (n + \alpha)\Delta t$ and the time step Δt meets the Nyquist condition: $\Delta t \leq \Delta t_{\text{nyq}} = \frac{1}{B}$. The parameter α controls the offset of the window edges with respect to the sample locations of the discrete data. The signal is not assumed to be synchronized with the sampling in any special way, so α is treated as a random variable with uniform distribution in the interval $[-\frac{1}{2}, \frac{1}{2}]$. It is not necessary to consider other values of α due to the stationarity of $s(t)$.

Our goal is to estimate the normalized mean square error, defined as

$$\epsilon^2 = \frac{E[|I - I_D|^2]}{E[|I|^2]}. \quad (8)$$

3. EVALUATION OF EXPECTATION VALUES

Using the Poisson summation formula and other standard Fourier identities, I and I_D can be rewritten in the forms:

$$I = T \int_{-\infty}^{\infty} S(\nu) W(T(\mu - \nu)) d\nu \quad (9)$$

and

$$I_D = T \sum_{n=-\infty}^{\infty} \int_{-\infty}^{\infty} S(\nu) W\left(T\left(\mu - \nu + \frac{n}{\Delta t}\right)\right) e^{2\pi i n \alpha} d\nu, \quad (10)$$

where $W(\nu)$ is the Fourier transform of the window function $w(\tau)$. Using the above equations and Equation (5), the desired expectation values may be computed:

$$E\left[|I - I_D|^2\right] = T^2 \sum_{\substack{n=-\infty \\ n \neq 0}}^{\infty} \int_{-\infty}^{\infty} \rho(\nu) \left|W\left(T\left(\mu - \nu + \frac{n}{\Delta t}\right)\right)\right|^2 d\nu \quad (11)$$

and

$$E\left[|I|^2\right] = T^2 \int_{-\infty}^{\infty} \rho(\nu) |W(T(\mu - \nu))|^2 d\nu. \quad (12)$$

4. LEADING ORDER ASYMPTOTICS

Up to this point, all results have been exact. The focus will now shift to the leading-order asymptotic behavior of Equation (8) when the window size T becomes large while the sampling spacing Δt and frequency μ are held constant.

Consider the denominator of Equation (8). Making the change of variables $\theta = T(\mu - \nu)$ in Equation (12) gives

$$\begin{aligned} E[|I|^2] &= T \int_{-\infty}^{\infty} \rho\left(\mu - \frac{\theta}{T}\right) |W(\theta)|^2 d\theta \\ &\sim T\rho(\mu^+) \int_{-\infty}^0 |W(\theta)|^2 d\theta + T\rho(\mu^-) \int_0^{\infty} |W(\theta)|^2 d\theta \end{aligned}$$

as $T \rightarrow \infty$. The notations $\rho(\mu^+)$ and $\rho(\mu^-)$ are to be understood as the limit of $\rho(\nu)$, $\nu \rightarrow \mu$ approaching from above and below, respectively. Since $w(\tau)$ is strictly real-valued, the Fourier transform has the symmetry $|W(\theta)|^2 = |W(-\theta)|^2$. The leading-order result can therefore be written as

$$E[|I|^2] \sim \frac{\rho(\mu^+) + \rho(\mu^-)}{2} T \int_{-\infty}^{\infty} w(\tau)^2 d\tau. \quad (13)$$

For the numerator of Equation (8), a different approach is necessary: an asymptotic expansion will be derived for $W(\nu)$, then plugged in to Equation (11). Note that $w(\tau)$ cannot be analytic for all τ since it is identically zero for $|\tau| > \frac{1}{2}$. It will be assumed that $w(\tau)$ is of order $p \geq 0$, meaning that:

1. $w^{(k)}(\tau)$ is differentiable everywhere for $k < p$;
2. $w^{(p)}(\tau)$ is differentiable everywhere, except possibly for a finite set of points $-\frac{1}{2} = \tau_1 < \tau_2 < \dots < \tau_L = \frac{1}{2}$;
3. $w^{(p)}(\tau)$ must be discontinuous at at least one of the τ_k , but not necessarily all of them.

It would be difficult to imagine any useful window function which does not meet the above conditions.

Next, write $W(\nu)$ in the form

$$W(\nu) = \sum_{k=1}^{L-1} \int_{\tau_k}^{\tau_{k+1}} w(\tau) e^{-2\pi i \nu \tau} d\tau.$$

Performing integration by parts repeatedly and collecting terms yields

$$W(\nu) = \frac{1}{(2\pi i \nu)^{p+1}} \sum_{k=1}^L e^{-2\pi i \nu \tau_k} \Delta w^{(p)}(\tau_k) + \frac{1}{(2\pi i \nu)^{p+1}} \sum_{k=1}^{L-1} \int_{\tau_k}^{\tau_{k+1}} e^{-2\pi i \nu \tau} w^{(p+1)}(\tau) d\tau, \quad (14)$$

where $\Delta w^{(p)}(\tau) \equiv w^{(p)}(\tau^+) - w^{(p)}(\tau^-)$. The Riemann-Lebesgue lemma [5] guarantees that the integrals on the right-hand side vanish as $\nu \rightarrow \infty$, so to leading order

$$W(\nu) \sim \frac{1}{(2\pi i\nu)^{p+1}} \sum_{k=1}^L e^{-2\pi i\nu\tau_k} \Delta w^{(p)}(\tau_k). \quad (15)$$

Inserting the asymptotic expression above into Equation (11) and keeping only terms of leading order as $T \rightarrow \infty$ yields:

$$E \left[|I - I_D|^2 \right] \sim \frac{\sum_{k=1}^L \Delta w^{(p)}(\tau_k)^2}{(2\pi T)^{2p}} \sum_{\substack{n=-\infty \\ n \neq 0}}^{\infty} \int_{-\infty}^{\infty} \frac{\rho(\nu)}{(\mu - \nu + \frac{n}{\Delta t})^{2p+2}} d\nu. \quad (16)$$

Note that in expanding $|W|^2$ via Equation (15), all terms where the complex exponentials do not cancel have been dropped. It can be shown via the Riemann-Lebesgue lemma that the dropped terms are of subleading order after integration over ν .

5. RESULTS FOR FLAT SPECTRAL DENSITY

To obtain an explicit formula for the error, let us assume that the random signal has a flat spectral density:

$$\rho(\nu) = \begin{cases} 1 & \text{if } |\nu| \leq \frac{B}{2} \\ 0 & \text{if } |\nu| > \frac{B}{2} \end{cases} \quad (17)$$

With a flat spectrum, the integrals in Equation (16) become trivial to evaluate analytically. Combining with Equation (13) produces the following asymptotic expression for the mean square error:

$$\epsilon^2 \sim \left(\frac{N_w}{N} \right)^{2p+1} F_p \left(\frac{\Delta t}{\Delta t_{\text{nyq}}}, 2\mu\Delta t \right) \text{ as } N \rightarrow \infty, \quad (18)$$

where

$$N = \frac{T}{\Delta t} \quad (19)$$

$$N_w = \left(\frac{\sum_{k=1}^L \Delta w^{(p)}(\tau_k)^2}{(2p+1)\pi^{2p+2} \int w(\tau)^2 d\tau} \right)^{\frac{1}{2p+1}} \quad (20)$$

$$F_p(x, y) = \frac{1}{2} (Q_p(x+y) + Q_p(x-y)) \quad (21)$$

$$Q_p(z) = \sum_{\substack{n=-\infty \\ n \neq 0}}^{\infty} \frac{1}{(2n-z)^{2p+1}}. \quad (22)$$

The quantities above all have simple interpretations. N is the number of samples in the window and is not required to be an integer. The choice of window function determines the order p and the constant N_w . The function F_p is independent of the window function; it determines the impact of the normalized sample spacing $\frac{\Delta t}{\Delta t_{\text{nyq}}}$ and scaled frequency $\mu\Delta t$.

5.1 EVALUATION OF $Q_p(Z)$

For $p > 0$, the sum in Equation (22) is absolutely convergent. For $p = 0$, the terms for positive and negative n may be combined, yielding a convergent series which is evaluated by the method of residues:

$$Q_0(z) = \sum_{\substack{n=-\infty \\ n \neq 0}}^{\infty} \frac{1}{2n-z} = \sum_{n=1}^{\infty} \frac{2z}{4n^2 - z^2} = \frac{1}{z} - \frac{\pi}{2} \cot \frac{\pi z}{2}. \quad (23)$$

Differentiating the above identity term-by-term with respect to z leads to analytic expressions

for Q_p , $p > 0$:

$$\begin{aligned} Q_1(z) &= \frac{1}{z^3} - \frac{1}{8}\pi^3 \cot\left(\frac{\pi z}{2}\right) \csc^2\left(\frac{\pi z}{2}\right) \\ Q_2(z) &= \frac{1}{z^5} - \frac{1}{192}\pi^5 (\cos(\pi z) + 5) \cot\left(\frac{\pi z}{2}\right) \csc^4\left(\frac{\pi z}{2}\right) \\ Q_3(z) &= \frac{1}{z^7} - \frac{\pi^7 (56 \cos(\pi z) + \cos(2\pi z) + 123) \cot\left(\frac{\pi z}{2}\right) \csc^6\left(\frac{\pi z}{2}\right)}{23040} \end{aligned}$$

It is also helpful to have a qualitative understanding of the behavior of $Q_p(z)$. Due to the restrictions $\Delta t \leq \Delta t_{\text{nyq}}$ and $|\mu| \leq \frac{B}{2}$, it is clear that only the range $0 \leq z \leq 2$ is relevant. From the definition in Equation (22), it is easy to demonstrate the following basic properties for all $p \geq 0$:

$$\begin{aligned} Q_p(0) &= 0 \\ Q_p(1) &= 1 \\ \lim_{z \rightarrow 2} Q_p(z) &= \infty \\ Q_p(z) &> 0 \quad \text{for } z > 0 \\ Q'_p(z) &> 0 \quad \text{for } z > 0 \\ Q''_p(z) &= (2p+1)(2p+2)Q_{p+1}(z). \end{aligned}$$

It directly follows that all derivatives of $Q_p(z)$ are positive for all $p \geq 0$, $z > 0$. The properties described above are easily seen in the plots of $Q_p(z)$ shown in Figure 1.

For $z \ll 1$, the analytic forms for $Q_p(z)$ given above become difficult to compute numerically due to the cancellation of diverging factors as $z \rightarrow 0$. Instead, it becomes simpler to compute using the Taylor series around $z = 0$:

$$Q_p(z) \approx \frac{(p + \frac{1}{2})\zeta(2p+2)}{4^p} z + \frac{(p + \frac{1}{2})(p+1)(p + \frac{3}{2})\zeta(2p+4)}{6 \cdot 4^p} z^3 + O(z^5), \quad (24)$$

where $\zeta(s) = \sum_{n=1}^{\infty} n^{-s}$ is the Riemann zeta function.

5.2 QUALITATIVE DESCRIPTION OF ERROR

The analysis above leads to the following general conclusions regarding the asymptotic error:

1. ϵ^2 decreases like $N^{-(2p+1)}$ for fixed Δt .
2. ϵ^2 decreases monotonically with Δt for fixed N .
3. ϵ^2 increases monotonically with $|\mu|$.
4. $\epsilon^2 \sim \left(\frac{N_{\text{nyq}}}{N}\right)^{2p+1}$ for $\mu = 0$ and critically sampled data.

5.3 EVALUATION OF N_w FOR STANDARD WINDOW FUNCTIONS

Table 1 list results for some of the most common window functions. For each window, the order p and constant N_w is shown. When possible, the exact analytic expression for N_w^{2p+1} is also given. In some cases, a second line in the table gives the next order term for the same window. The order p is determined by consecutively examining $w(\tau)$ and its derivatives until a discontinuity is found. The constant N_w is then computed directly from Equation (20). All analytic and numeric results were generated using Mathematica 5.2.

It should be stressed that the results for next-to-leading order terms in Table 1 are, strictly speaking, not the next term in a correct asymptotic expansion. Instead, they are simply the result obtained by pretending that the leading order N_w is zero, and continuing with the leading-order analysis to larger p until a non-zero term is obtained. This is useful mainly in cases where the true leading order N_w is numerically very small, such as in the case of the Hamming window.

5.4 VERIFICATION OF ASYMPTOTIC RESULTS

Since the results derived are asymptotic in N , there is no guarantee that they will achieve any specific level of accuracy except in the limit $N \rightarrow \infty$. To establish the utility of the asymptotic formula, the normalized error was computed via Monte Carlo with 10^5 random trials. Random data was generated with the required correlation properties at a sample spacing of $\frac{\Delta t}{20}$. The integral in Equation (6) was approximated using the highly oversampled data. The sum in Equation (7) was computed directly using every 20th sample. Averaging over values of α was approximated by a discrete average over the values $\alpha = 0, \frac{1}{20}, \frac{2}{20}, \dots, \frac{19}{20}$. The Monte Carlo results were then compared with the theoretical asymptotic predictions from Equation (18).

In Figures 2 and 3, the errors are shown as a function of number of samples for the square, triangle, Hamming, Reisz, and Bohman windows. For these examples, the frequency is $\mu = 0$ and sampling rate is $\Delta t / \Delta t_{\text{nyq}} = 0.8$. The agreement between Monte Carlo and the asymptotic curves appears to be excellent, even down to very small numbers of samples. In particular, the square window results match Monte Carlo closely even for a single sample.

For the Hamming and Kaiser windows, the leading order coefficient N_w is very small. Consequently, convergence to the asymptotic result requires larger values of N . Figures 4 and 5 compare Monte Carlo results with leading order asymptotics as well as leading plus subleading order. The subleading term appears to improve the results for small N , but by $N = 5$ the leading term suffices.

In Figure 6, errors are shown as a function of frequency for the square, triangle, and Hamming windows. The number of samples is fixed at $N = 10$ in all cases. The asymptotic error increases monotonically with $|\mu|$, as described earlier in Section 5.2. While the agreement is good near zero frequency, it appears that the asymptotic formula overestimates the error near the Nyquist limit, especially for the triangle and Hamming windows. This is not surprising, since the asymptotic formula ceases to be valid past the Nyquist limit.

TABLE 1
Parameters for Some Standard Window Functions

Name	$w(\tau)$ for $ \tau \leq \frac{1}{2}$	p	N_w^{2p+1}	N_w
square	1	0	$\frac{2}{\pi^2}$	0.2026
triangle	$1 - 2 \tau $	1	$\frac{24}{\pi^4}$	0.6269
Reisz	$1 - 4\tau^2$	1	$\frac{20}{\pi^4}$	0.5899
Hamming	$0.54 + 0.46 \cos(2\pi\tau)$	0	$\frac{64}{1987\pi^2}$	0.003263
		2	$\frac{33856}{9935\pi^2}$	0.8084
Hanning	$0.5 + 0.5 \cos(2\pi\tau)$	2	$\frac{64}{15\pi^2}$	0.8456
Blackman	$0.42 + 0.5 \cos(2\pi\tau) + 0.08 \cos(4\pi\tau)$	2	$\frac{5184}{7615\pi^2}$	0.5858
Bohman	$(1 - 2 \tau) \cos(2\pi\tau) + \frac{1}{\pi} \sin(2\pi \tau)$	3	$\frac{18432}{7\pi^2(15+2\pi^2)}$	1.338
Kaiser ($\beta=1$)	$\frac{I_0(\sqrt{1-4\tau^2})}{I_0(1)}$	0		0.1460
Kaiser ($\beta=3$)	$\frac{I_0(3\sqrt{1-4\tau^2})}{I_0(3)}$	0		0.01599
		1		0.3523
Kaiser ($\beta=5$)	$\frac{I_0(5\sqrt{1-4\tau^2})}{I_0(5)}$	0		0.000677
		1		0.2426

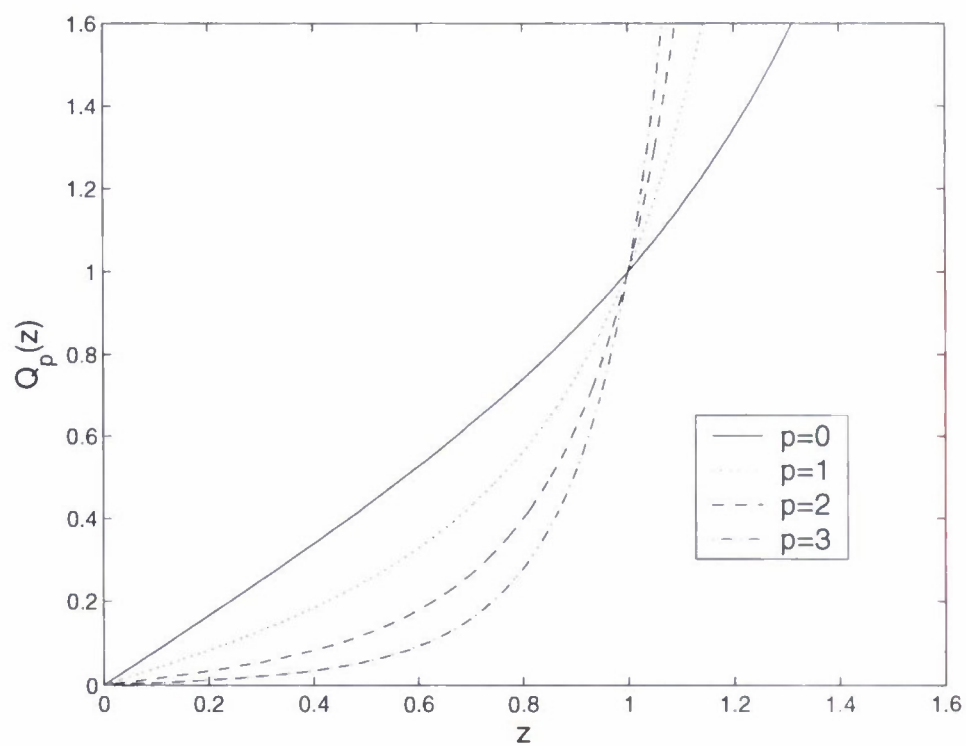


Figure 1. Plot of the function $Q_p(z)$.

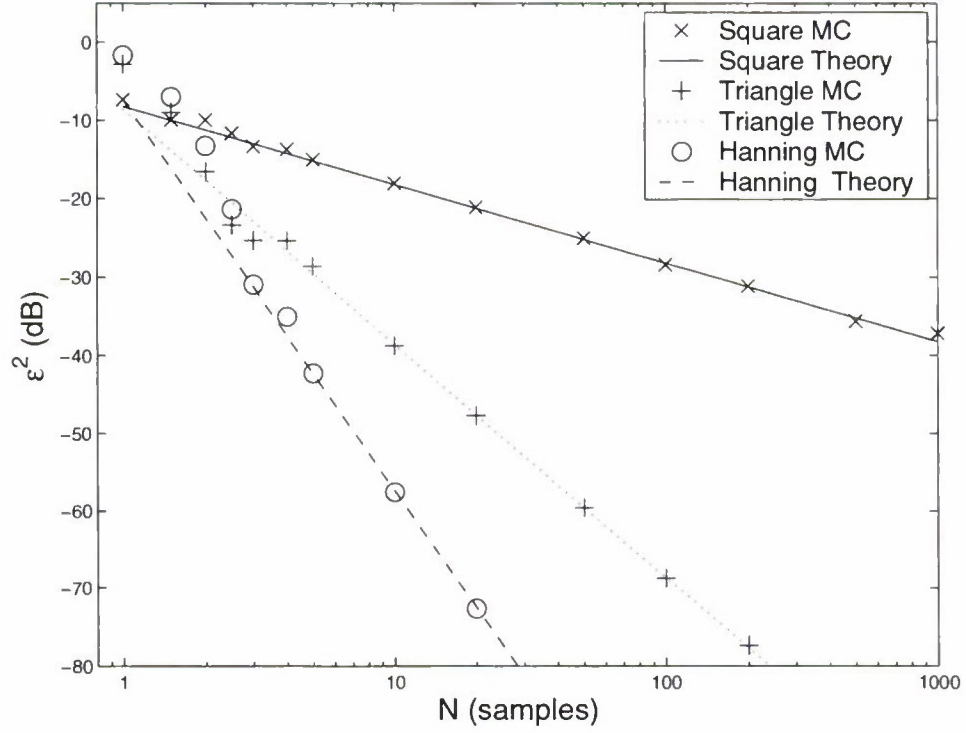


Figure 2. Normalized mean squared error versus number of samples in window. Results are shown for both Monte Carlo and the asymptotic error formula in Equation (18). All results are for zero frequency ($\mu = 0$) and sampling rate of $\Delta t / \Delta t_{\text{nyq}} = 0.8$.

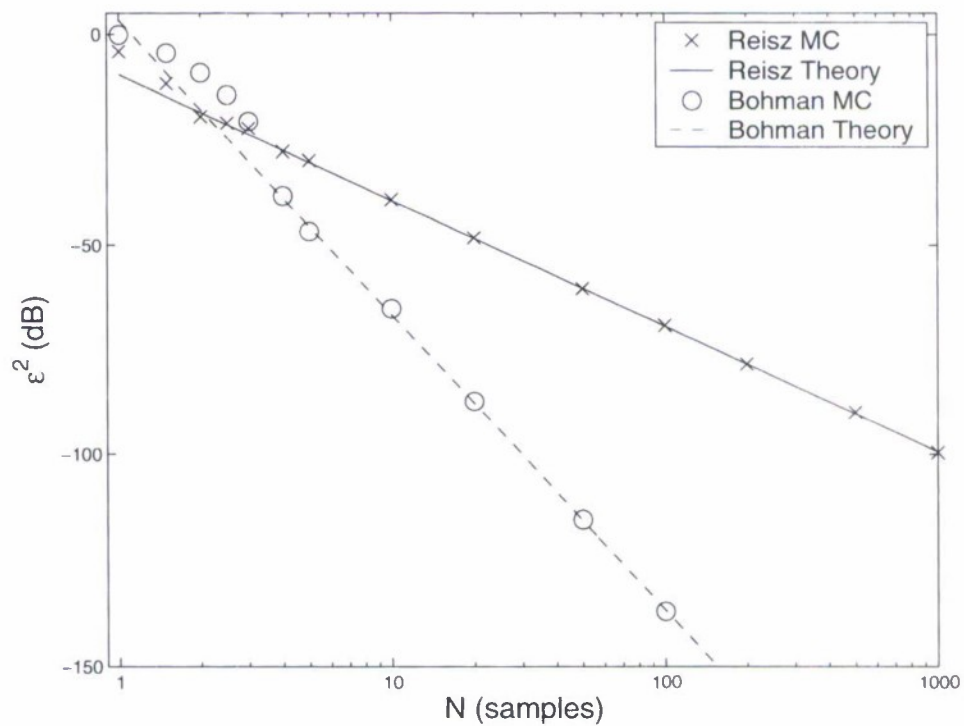


Figure 3. Normalized mean squared error versus number of samples in window. Results are shown for both Monte Carlo and the asymptotic error formula in Equation (18). All results are for zero frequency ($\mu = 0$) and sampling rate of $\Delta t / \Delta t_{\text{nyq}} = 0.8$.

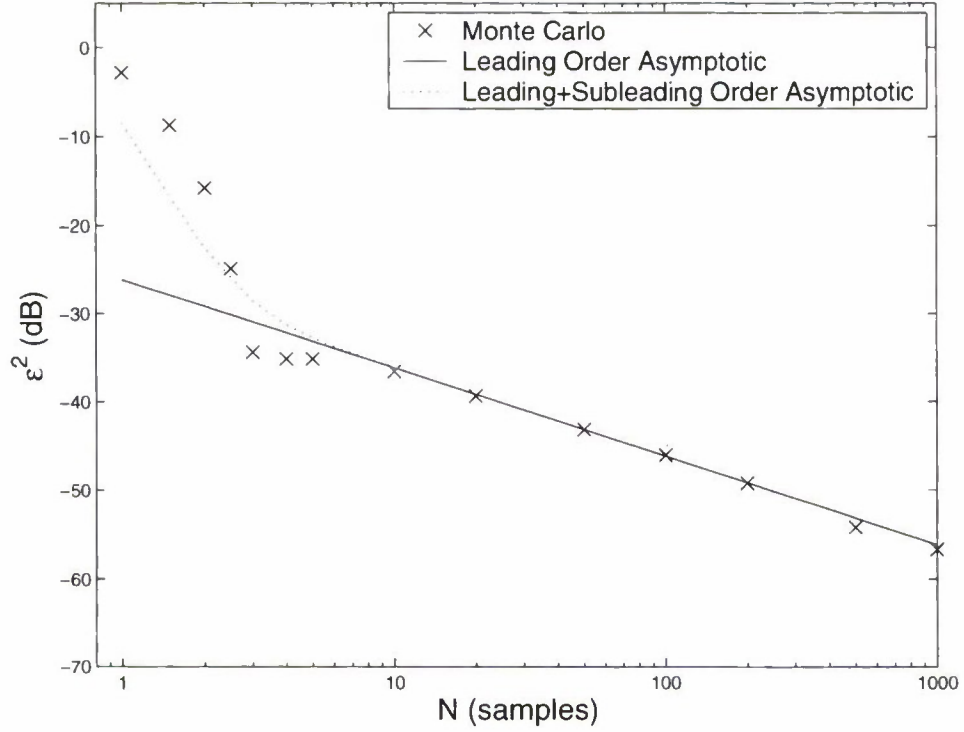


Figure 4. Normalized mean squared error for the Hamming window. Results are shown using both Monte Carlo and the asymptotic error formula in Equation (18). Asymptotic results are shown for both leading order and leading plus subleading order. All cases are for zero frequency ($\mu = 0$) and sampling rate of $\Delta t / \Delta t_{\text{nyq}} = 0.8$.

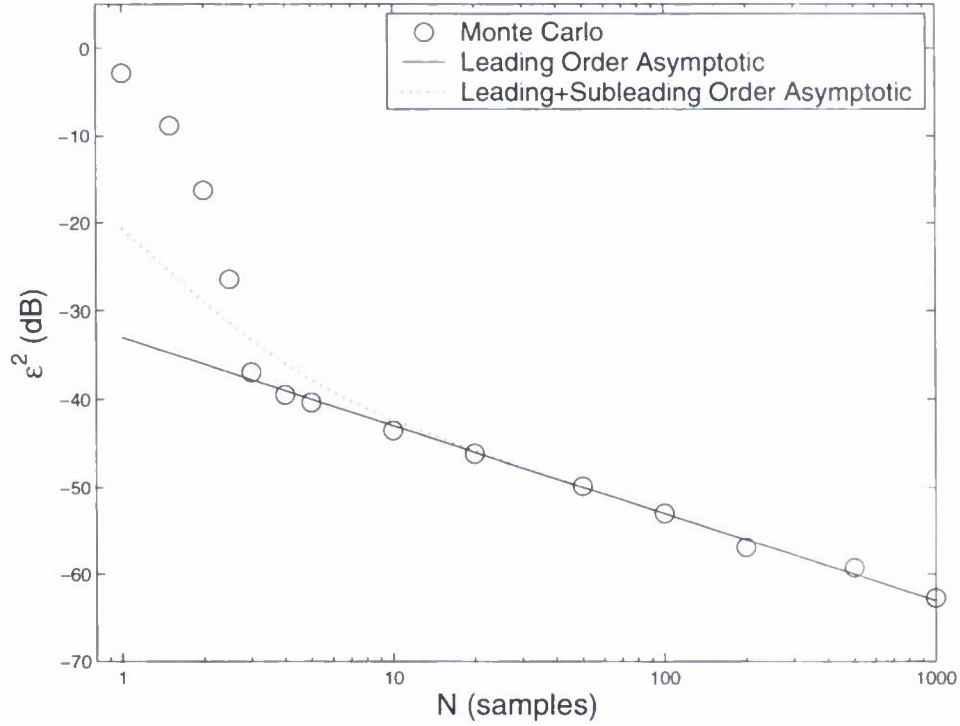


Figure 5. Normalized mean squared error for the Kaiser window ($\beta = 5$). Results are shown using both Monte Carlo and the asymptotic error formula in Equation (18). Asymptotic results are shown for both leading order and leading plus subleading order. All cases are for zero frequency ($\mu = 0$) and sampling rate of $\Delta t / \Delta t_{\text{nyq}} = 0.8$.

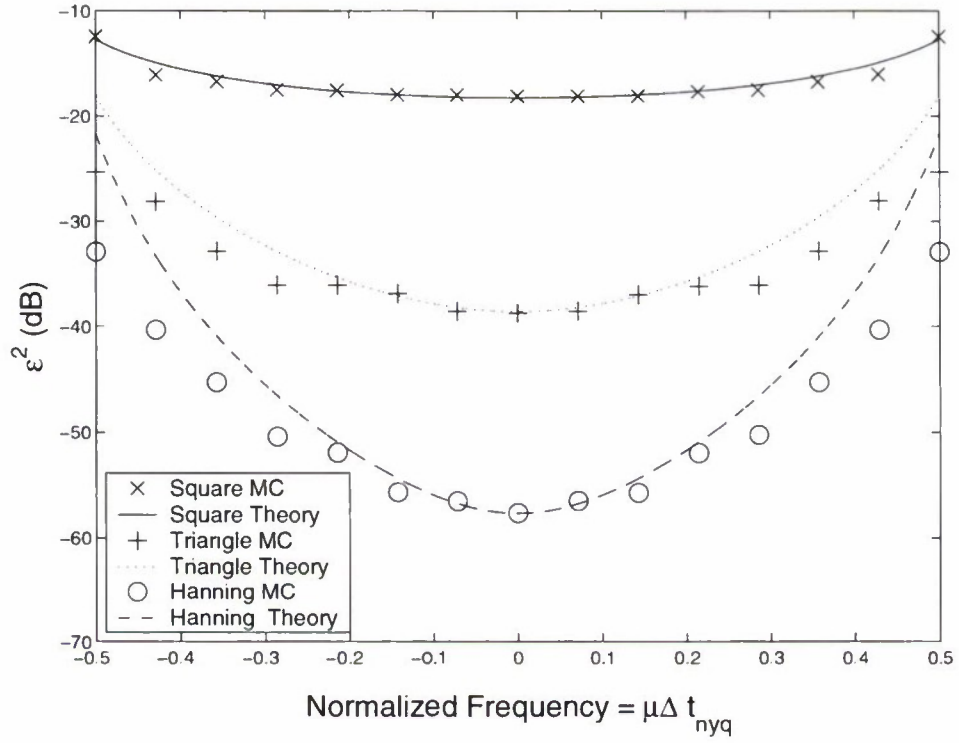


Figure 6. Normalized mean squared error versus frequency. Results are shown using both Monte Carlo and the asymptotic error formula in Equation (18). All cases are for $N = 10$ samples and sampling rate of $\Delta t/\Delta t_{nyq} = 0.8$.

6. CONCLUSIONS

The windowed DFT can be regarded as an approximation of the continuous Fourier transform with the same window function. The mean square error for stochastic signals is for the most part accurately captured by the asymptotic formula in Equation (18). Parameters for some of the most common window functions are tabulated in Table 1. Monte Carlo calculations confirm that the asymptotic error is accurate, even when the number of samples N is small. Deviations from the asymptotic result mainly occur for frequencies approaching the Nyquist limit.

The asymptotic error formula should prove especially useful in scenarios where the processing parameters must be determined dynamically during processing. In such cases, the asymptotic result permits one to analytically optimize any design metric.

APPENDIX A

MATHEMATICA CODE FOR GENERATING ASYMPTOTIC RESULTS

The results presented in Table 1 were prepared using Mathematica version 5.2. Figure A-1 shows the actual commands used to generate the results, along with comments to indicate the purpose of various steps. Inputs to Mathematica are indicated in bold type, while outputs and comments are in normal type.

Calculations for Asymptotic Error in DFT

Define oversampling error function:

```
q[p_, x_] :=  
Sum[1 / (2 n - x) ^ (2 p + 1) - 1 / (2 n + x) ^ (2 p + 1), {n, 1, Infinity}] // FullSimplify
```

Compute first few cases:

q[0, x]

$$\frac{1}{x} - \frac{1}{2} \pi \cot\left[\frac{\pi x}{2}\right]$$

q[1, x]

$$\frac{1}{x^3} - \frac{1}{8} \pi^3 \cot\left[\frac{\pi x}{2}\right] \operatorname{Csc}\left[\frac{\pi x}{2}\right]^2$$

q[2, x]

$$\frac{1}{x^5} - \frac{1}{192} \pi^5 (5 + \cos[\pi x]) \cot\left[\frac{\pi x}{2}\right] \operatorname{Csc}\left[\frac{\pi x}{2}\right]^4$$

q[3, x]

$$\frac{1}{x^7} - \frac{\pi^7 (123 + 56 \cos[\pi x] + \cos[2 \pi x]) \cot\left[\frac{\pi x}{2}\right] \operatorname{Csc}\left[\frac{\pi x}{2}\right]^6}{23040}$$

q[4, x]

$$\frac{1}{x^9} - \frac{\pi^9 (5786 + 4047 \cos[\pi x] + 246 \cos[2 \pi x] + \cos[3 \pi x]) \cot\left[\frac{\pi x}{2}\right] \operatorname{Csc}\left[\frac{\pi x}{2}\right]^8}{5160960}$$

q[5, x]

$$\frac{1}{x^{11}} - \frac{1}{1857945600} \left(\pi^{11} (450995 + 408364 \cos[\pi x] + 46828 \cos[2 \pi x] + 1012 \cos[3 \pi x] + \cos[4 \pi x]) \cot\left[\frac{\pi x}{2}\right] \operatorname{Csc}\left[\frac{\pi x}{2}\right]^{10} \right)$$

Define window functions for $-1/2 < x < 1/2$:

```
square[x_] := 1
```

```
hanning[x_] := 1/2 + (1/2) Cos[2 * Pi * x]
```

```
hamming[x_] := (54/100) + (46/100) * Cos[2 * Pi * x]
```

```
blackman[x_] := 42/100 + (50/100) Cos[2 * Pi * x] + (8/100) * Cos[4 * Pi * x]
```

Figure A-1. Transcript of Mathematica.

```

abs[x_] := Piecewise[{{-x, x < 0}, {x, x ≥ 0}}]

General::spell1: Possible spelling error: new symbol name "abs" is similar to existing symbol "Abs". More...

triangle[x_] := 1 - 2*abs[x]

reisx[x_] := 1 - 4 x^2

bohman[x_] := (1 - 2 abs[x]) Cos[2 Pi x] + (1 / Pi) Sin[2 Pi abs[x]]

kaiser[β_][x_] := BesselI[0, β Sqrt[1 - (2 x)^2]] / BesselI[0, β]

```

Define functions to compute leading order error term:

```

disc[f_] := Module[{g, x, s},
  g[y_] =
    (Limit[f[x], x -> y, Direction -> -1] - Limit[f[x], x -> y, Direction -> 1]) // Simplify;
  s = Solve[Reduce[g[x] != 0, x], x];
  Limit[f[x], x -> 1/2]^2 +
    Limit[f[x], x -> -1/2]^2 + If[Length[s] > 0, Total[{g[x] /. s}^2], 0]
]

err[g0_] := Module[{x, norm, g, coef, p, p2, temp, temp2},
  norm = Integrate[g0[x]^2, {x, -1/2, 1/2}];
  g[x_] = g0[x];
  coef = disc[g];
  p = 0;
  While[coef == 0,
    g[x_] = FullSimplify[D[g[x], x], x ∈ Reals]; coef = disc[g]; p = p + 1;
    temp = Simplify[(coef / (norm * (2 p + 1) * Pi^(2 + p + 2)))];
    g[x_] = FullSimplify[D[g[x], x], x ∈ Reals];
    {p, temp, N[temp^(1 / (2 p + 1))]}
  ]
]

```

Define function to compute first two leading error terms:

```

err2[g0_] := Module[{x, norm, g, coef, p, p2, temp, temp2},
  norm = Integrate[g0[x]^2, {x, -1/2, 1/2}];
  g[x_] = g0[x];
  coef = disc[g];
  p = 0;
  While[coef == 0,
    g[x_] = FullSimplify[D[g[x], x], x ∈ Reals]; coef = disc[g]; p = p + 1;
    temp = Simplify[(coef / (norm * (2 p + 1) * Pi^(2 + p + 2)))];
    g[x_] = FullSimplify[D[g[x], x], x ∈ Reals];
    coef = disc[g];
    p2 = p + 1;
    While[coef == 0,
      g[x_] = FullSimplify[D[g[x], x], x ∈ Reals]; coef = disc[g]; p2 = p2 + 1;
      temp2 = Simplify[(coef / (norm * (2 p2 + 1) * Pi^(2 + p2 + 2)))];
      {p, temp, N[temp^(1 / (2 p + 1))], p2, temp2, N[temp2^(1 / (2 p2 + 1))]}
    ]
  ]
]

```

Figure A-1. Transcript of Mathematica (continued).

Compute results:

```

err[square]
{0,  $\frac{2}{\pi^2}$ , 0.202642}

err2[hanning]
{2,  $\frac{64}{15 \pi^2}$ , 0.845586, 4,  $\frac{1024}{27 \pi^2}$ , 1.16134}

err2[hamming]
{0,  $\frac{64}{1987 \pi^2}$ , 0.00326349, 2,  $\frac{33856}{9935 \pi^2}$ , 0.808414}

err2[blackman]
{2,  $\frac{5184}{7615 \pi^2}$ , 0.585786, 4,  $\frac{173056}{1523 \pi^2}$ , 1.31193}

err2[reisz]
{1,  $\frac{20}{\pi^4}$ , 0.589943, 2,  $\frac{48}{\pi^6}$ , 0.549121}

err[triangle]
{1,  $\frac{24}{\pi^4}$ , 0.626908}

err2[bohman]
{3,  $\frac{18432}{7 \pi^2 (15 + 2 \pi^4)}$ , 1.33807, 5,  $\frac{1179648}{165 \pi^2 + 22 \pi^4}$ , 1.68593}

err2[kaiser[1]]
{0,  $\frac{2}{\pi^2 \text{BesselI}[0, 1]^2} \int_{-\frac{1}{2}}^{\frac{1}{2}} \frac{\text{BesselI}[0, \sqrt{1-4 x^2} 183198]}{\text{BesselI}[0, 1]^2} dx$  183198, 0.146048,
1,  $\frac{2}{3 \pi^4 \text{BesselI}[0, 1]^2} \int_{-\frac{1}{2}}^{\frac{1}{2}} \frac{\text{BesselI}[0, \sqrt{1-4 x^2} 183198]}{\text{BesselI}[0, 1]^2} dx$  183198, 0.170226}

err2[kaiser[2]]
{0,  $\frac{2}{\pi^2 \text{BesselI}[0, 2]^2} \int_{-\frac{1}{2}}^{\frac{1}{2}} \frac{\text{BesselI}[0, 2 \sqrt{1-4 x^2} 184468]}{\text{BesselI}[0, 2]^2} dx$  184468, 0.0588426,
1,  $\frac{32}{3 \pi^4 \text{BesselI}[0, 2]^2} \int_{-\frac{1}{2}}^{\frac{1}{2}} \frac{\text{BesselI}[0, 2 \sqrt{1-4 x^2} 184468]}{\text{BesselI}[0, 2]^2} dx$  184468, 0.316809}

```

Figure A-1. Transcript of Mathematica (continued).

```
err2[kaiser[3]]
```

$$\left\{ 0, \frac{2}{\pi^2 \text{BesselI}[0, 3]^2} \int_{-\frac{1}{2}}^{\frac{1}{2}} \frac{\text{BesselI}[6, 3 \sqrt{1-4 x^2 185736}]}{\text{BesselI}[0, 3]^2} dx \$185736, 0.0159883, \right.$$

$$\left. 1, \frac{54}{\pi^4 \text{BesselI}[0, 3]^2} \int_{-\frac{1}{2}}^{\frac{1}{2}} \frac{\text{BesselI}[6, 3 \sqrt{1-4 x^2 185736}]}{\text{BesselI}[0, 3]^2} dx \$185736, 0.352335 \right\}$$

```
err2[kaiser[4]]
```

$$\left\{ 0, \frac{2}{\pi^2 \text{BesselI}[0, 4]^2} \int_{-\frac{1}{2}}^{\frac{1}{2}} \frac{\text{BesselI}[6, 4 \sqrt{1-4 x^2 187004}]}{\text{BesselI}[0, 4]^2} dx \$187004, 0.003492, \right.$$

$$\left. 1, \frac{512}{3 \pi^4 \text{BesselI}[0, 4]^2} \int_{-\frac{1}{2}}^{\frac{1}{2}} \frac{\text{BesselI}[6, 4 \sqrt{1-4 x^2 187004}]}{\text{BesselI}[0, 4]^2} dx \$187004, 0.311385 \right\}$$

```
err2[kaiser[5]]
```

$$\left\{ 0, \frac{2}{\pi^2 \text{BesselI}[0, 5]^2} \int_{-\frac{1}{2}}^{\frac{1}{2}} \frac{\text{BesselI}[6, 5 \sqrt{1-4 x^2 188272}]}{\text{BesselI}[0, 5]^2} dx \$188272, 0.000677044, \right.$$

$$\left. 1, \frac{1250}{3 \pi^4 \text{BesselI}[0, 5]^2} \int_{-\frac{1}{2}}^{\frac{1}{2}} \frac{\text{BesselI}[6, 5 \sqrt{1-4 x^2 188272}]}{\text{BesselI}[0, 5]^2} dx \$188272, 0.242675 \right\}$$

Figure A-1. Transcript of Mathematica (continued).

REFERENCES

- [1] L. Cohen, *Time-Frequency Analysis*. Upper Saddle River, NJ: Prentice-Hall, 1995.
- [2] J. W. McCorkle and M. Rofheart, "Order $N^2 \log(N)$ backprojector algorithm for focusing wide-angle wide-bandwidth arbitrary-motion synthetic aperture radar," in *Proc. SPIE Radar Sensor Technology*, G. S. Ustach, Ed., vol. 2747, no. 1, Orlando, FL, USA, June 1996, pp. 25-36.
- [3] A. F. Yegulalp, "Fast backprojection algorithm for synthetic aperture radar," in *Proc. IEEE Radar Conference*, Waltham, MA, Apr. 1999, pp. 60-65.
- [4] R. I. Becker and N. Morrison, "The errors in FFT estimation of the Fourier transform," *IEEE Trans. Signal Processing*, vol. 44, no. 8, pp. 2073-2077, Aug. 1996.
- [5] C. M. Bender and S. Orszag, *Advanced Mathematical Methods for Scientists and Engineers*. New York: McGraw-Hill, 1978.

REPORT DOCUMENTATION PAGE				Form Approved OMB No. 0704-0188	
Public reporting burden for this collection of information is estimated to average 1 hour per response, including the time for reviewing instructions, searching existing data sources, gathering and maintaining the data needed, and completing and reviewing this collection of information. Send comments regarding this burden estimate or any other aspect of this collection of information, including suggestions for reducing this burden to Department of Defense, Washington Headquarters Services, Directorate for Information Operations and Reports (0704-0188), 1215 Jefferson Davis Highway, Suite 1204, Arlington, VA 22202-4302. Respondents should be aware that notwithstanding any other provision of law, no person shall be subject to any penalty for failing to comply with a collection of information if it does not display a currently valid OMB control number. PLEASE DO NOT RETURN YOUR FORM TO THE ABOVE ADDRESS.					
1. REPORT DATE (DD-MM-YYYY) 08-25-2006		2. REPORT TYPE Technical Report		3. DATES COVERED (From - To)	
4. TITLE AND SUBTITLE Asymptotic Error for Windowed Discrete Fourier Transforms				5a. CONTRACT NUMBER FA8721-05-C-0002	
				5b. GRANT NUMBER	
				5c. PROGRAM ELEMENT NUMBER	
6. AUTHOR(S) A.F. Yegulalp				5d. PROJECT NUMBER 741	
				5e. TASK NUMBER 11	
				5f. WORK UNIT NUMBER	
7. PERFORMING ORGANIZATION NAME(S) AND ADDRESS(ES) MIT Lincoln Laboratory 244 Wood Street Lexington, MA 02420-9108				8. PERFORMING ORGANIZATION REPORT NUMBER TR-1107	
9. SPONSORING / MONITORING AGENCY NAME(S) AND ADDRESS(ES) Defense Advanced Research Projects Agency, IXO 3701 N. Fairfax Drive Arlington, VA 22203-1714				10. SPONSOR/MONITOR'S ACRONYM(S)	
				11. SPONSOR/MONITOR'S REPORT NUMBER(S) ESC-TR-2005-068	
12. DISTRIBUTION / AVAILABILITY STATEMENT Approved for public release; distribution is unlimited.					
13. SUPPLEMENTARY NOTES					
14. ABSTRACT The windowed discrete Fourier transform (DFT) is a widely used tool in countless signal processing applications. Surprisingly, there has been little analysis of the accuracy for the processing of random bandlimited signals. This report derives an error formula at leading asymptotic order in the number of data samples. The formula applies to essentially any window function, with explicit results tabulated for some of the most common cases. The asymptotic error is shown to agree well with Monte Carlo results, even for very small numbers of samples.					
15. SUBJECT TERMS					
16. SECURITY CLASSIFICATION OF:			17. LIMITATION OF ABSTRACT	18. NUMBER OF PAGES	19a. NAME OF RESPONSIBLE PERSON
a. REPORT Unclassified	b. ABSTRACT Unclassified	c. THIS PAGE Unclassified			19b. TELEPHONE NUMBER (include area code)
			None	36	